

Doppler imaging of stellar surfaces - techniques and issues

J.B. RICE

Brandon University, Brandon, MB, R7A 6A9 Canada

Received 2002 May 10; accepted 2002 July 3

Abstract. The development of Doppler imaging has allowed us to observe stellar activity on the surface of stars other than the Sun for over a decade. We are now in a position to compare activity on rapidly rotating T Tauri, RS CVn and young main-sequence stars and to compare the activity on those, in turn, with that of the Sun. The images produced show some startling differences between stellar and solar activity. The strengths and weakness of the Doppler imaging technique must be reviewed regularly to remind us of what observed features are reliable and of when we should have doubts. This review is a general survey of the technique emphasizing the issue of testing and of potential artifacts without attempting excessive detail on variations in application or results. The difficulties faced as the technique is extended from images of surface temperature or abundance to images that include magnetic information are briefly surveyed.

Key words: techniques: spectroscopic – methods: numerical – stars: spots – stars: activity

1. Background

1.1. History and outline

A few years ago discussion of spots on stars would have consisted of a discussion of solar activity and little else. The last few decades have seen various techniques developed to extend the high resolution frontier in astronomy. Interferometry, space telescopes and active optics for ground telescopes have all played their role in improving spatial resolution on the sky but probably the greatest increase in effective resolution has been from the application of Doppler imaging (DI). Radio long-baseline interferometry may give us milliarcsecond resolution but Doppler imaging can reach an effective resolution several orders of magnitude better than that. The application of DI over the last decade has produced images of many stars for comparison with the Sun and with the theories of stellar activity. For those unfamiliar with Doppler imaging, I present this general survey as a preliminary to having papers following this on some of the results we have enjoyed in the last decade.

The foundations of DI were laid, primarily by Russian astronomers working on abundance maps of Ap stars in the 1970s (Goncharski et al. 1977; Rice et al. 1981). Through the 1980s these techniques came to be applied to cool stars and images of surface spots. Vogt et al. (1987) marked the beginning of the full application of DI to spot imaging. Over the last decade the widespread application of DI has produced abundant images and some aspects of the images have given

Correspondence to: rice@brandonu.ca

rise to doubts about the reliability of specific types of features. The potential for generating artifacts in DI reconstructions have led some of us to run tests comparing the reconstruction of images from artificial data, where incorrect parameters have been used in the reconstruction, with the original images to test for the conditions that might lead to the production of artifacts. On rare occasions we have had images from real data where the reconstruction was done independently by different groups and that has given us the chance to intercompare the results from different DI codes given identical real data for input. On at least one occasion, data has been collected independently and simultaneously on the same star and the reconstructions computed and published with absolutely no interaction between the teams. This gives an ideal “double blind” type of test of reliability.

Here I will review some of the differences in DI techniques, some of the work done on testing the techniques and comment on my impressions of the reliability of arguable features such as polar caps and plages. I will finish with some comments on the efforts to reach the holy grail of imaging, the simultaneous imaging of spots and magnetic fields from spectra obtained in both I and V or perhaps even in all four Stokes polarization components I, Q, U and V.

1.2. The basic techniques for DI

The foundation of Doppler imaging is the distinctive manner in which spots at varying locations on the surface of the star produce deviations from the ideal rotationally broadened line profile. A localized cool spot will produce a “bump” toward

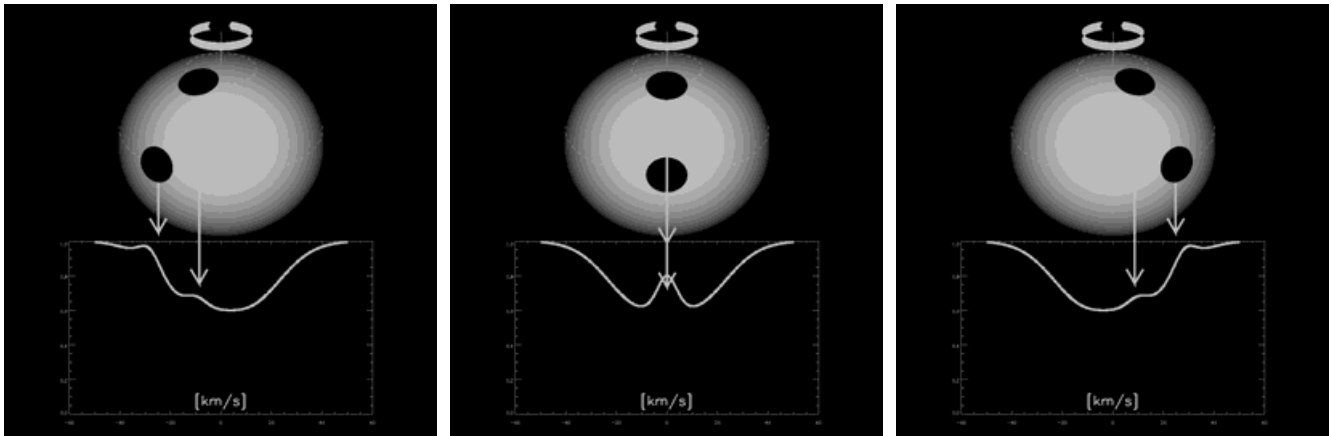


Fig. 1. The basis of Doppler imaging. The behaviour of the "bump" produced in the spectra of stars by cool spots on the stellar surface is very different over time depending on both the longitude and latitude of the spot on the stellar surface.

the level of the continuum in the observed spectrum compared with the ideal profile of an unblemished star surface. The behaviour of this "bump" with time will establish both its longitude and its latitude as illustrated in Fig. 1. Spots near the stellar equator will produce a "bump" that is only visible for half the rotational cycle of the star and that migrates with time from the extreme blue wing of the line profile to the extreme red. Higher latitude spots produce bumps that may be visible all the time and that will migrate back and forth near line centre as the star rotates.

The mathematical process of Doppler imaging is essentially always a matter of creating an error function that represents the degree to which the predicted spectrum from a current trial image of a star (the forward calculation) differs from the observed spectrum and then iteratively reducing the error function to a minimum consistent with the error of the observations. Typically the error function is represented as:

$$E = \sum_{\phi} \sum_{\lambda} \frac{1}{\sigma_{\lambda, \phi}^2} [R_{calc}(\lambda, \phi) - R_{obs}(\lambda, \phi)]^2 + \alpha f \quad (1)$$

or in shorter form this may be written as:

$$E = \chi^2 + \alpha f. \quad (2)$$

Here R_{calc} represents the predicted line spectrum from the forward calculation and R_{obs} represents the observed spectrum. The $\sigma_{\lambda, \phi}$ represents the error of the individual observations. The squared difference between the forward calculation and the observation is summed over all wavelengths and a full set of observations spaced in time through the full cycle of phases, ϕ , of the star's rotation. Some of the techniques used in basic DI have been reviewed in Piskunov & Rice (1993). The evolution of techniques was essentially from the initial use of analytical shapes for local line profiles, such as the Minnaert profile used in Goncharski et al. (1982), with minimization through conjugate gradients. An alternative to using analytical expressions for the line shapes was to use a fixed empirical local line profile (Vogt et al. 1987) which allows a linearized forward calculation. Using a linearized

forward calculation, where the image vector is related to the calculated profile by a transformation matrix that incorporates the stellar geometry, permitted use of a matrix inversion procedure written by Skilling and Gull called MEMSYS (see for example Skilling & Bryan 1984). Subsequent techniques have replaced the analytical or empirical local line profiles with profiles calculated from model atmospheres appropriate to the local conditions on the image. Calculating the line profiles for every element of the surface for each iteration of the conjugate gradient minimization routine would demand an inordinate amount of computing time so the profile calculations are tabled for an array of limb angles and temperatures as outlined in Piskunov & Rice (1993).

As a dramatic example of extreme line profile variations and the resultant map I include Fig. 2 showing the oxygen triplet at 7775Å and the map of oxygen abundance over the surface of ϵ UMa. Certainly, in the extreme case, Doppler imaging works well but what about the effects in the case of less dramatic profile and temperature variations.

2. The basic variations in Doppler imaging technique

2.1. The regularization

The function $f(\theta, l)$ in Eqn. 1 is a regularizing function whose role is to limit E so that the minimization does not produce an image with detail such that E is reduced below the formal error in the observed profiles. Since the local line profile is usually wide enough to affect multiple pixels in the observed spectrum, the tendency is for the process of minimizing the expression for E, even without the effect of f, to produce a smoothed image. Hendry & Mochnacki (2000) have given a good explanation of why distribution of the effect of the local profile from one pixel over many observed data points produces a natural smoothing in the image. Nonetheless, more structure than is justified by the total photon noise

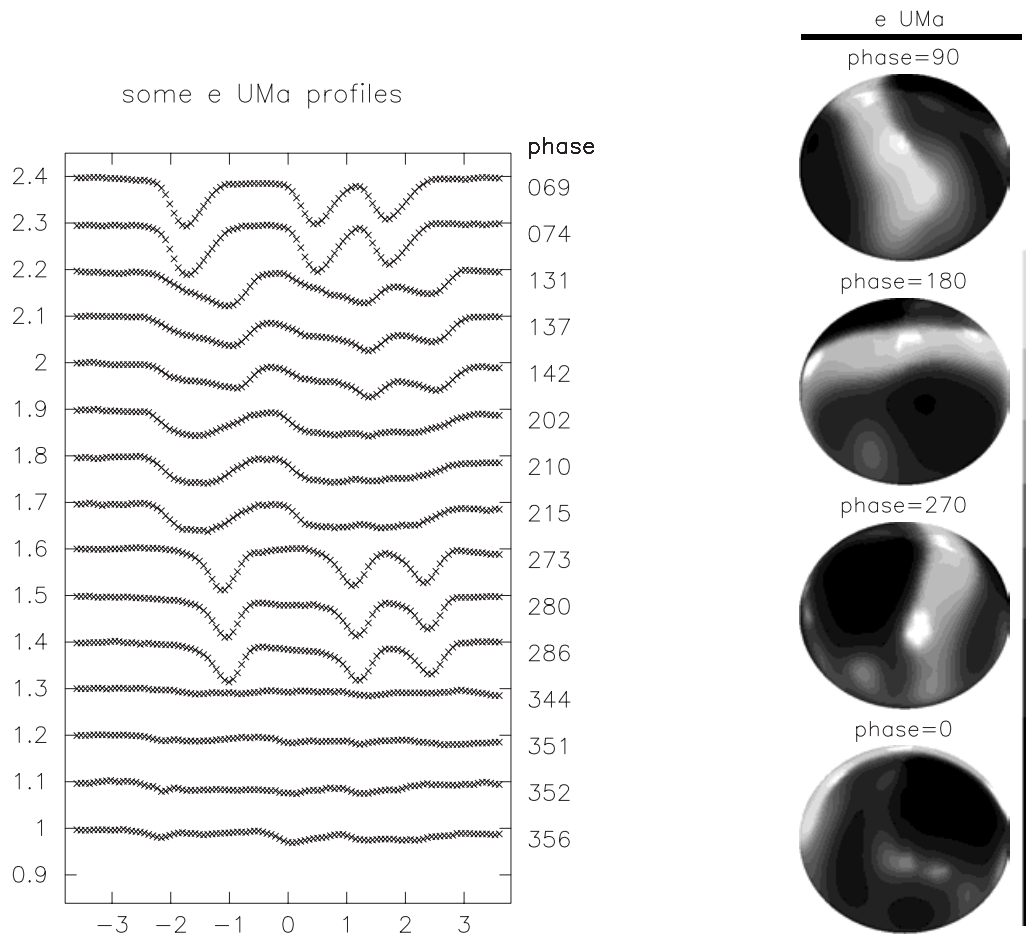


Fig. 2. The dramatic line profile variations of the oxygen triplet lines at 7775\AA are shown on the left. The x-axis is wavelength in Angstroms measured from the centre of the line system. The derived, very extreme abundance depletion of oxygen in a wide region around the magnetic pole of ϵ UMa is shown in four successive spherical projections of the oxygen map of ϵ UMa on the right. The abundance variation is from normal solar abundances in the bright belt at the magnetic equator to five orders of magnitude less in the dark regions of the magnetic poles.

plus external error may appear in the image. Since, without a regularizing function, the minimization of χ^2 by itself may tend to over fit the data, some additional penalty for excess detail must be provided in the error function. The effect of the regularizing function is modulated by a Lagrangian multiplier “ α ” in Equ. 1 so that the resultant image will just fit the observed profiles to the formal error in the data. Two forms of regularizing function have been in widespread use. One is the Tikhonov (1963) function (Equ. 3) where the function is based on the square difference from point to point on the surface of the star. The Tikhonov function is designed to simply smooth the image. The other widely used regularizing function is the maximum entropy function (Equ. 4) where the effect of the regularizing function is to drive the solution to a mean value in the absence of information in the observed profiles that would force the solution away from the mean.

$$f = \int_{-\pi}^{\pi} \int_{-\pi/2}^{\pi/2} \left[\left(\frac{\partial T}{\partial \theta} \right)^2 + \left(\frac{\partial T}{\partial l} \right)^2 \right] d\theta dl \quad (3)$$

The Tikhonov regularizing function is probably the best a priori choice for Ap star work and the maximum entropy function may well be the best a priori choice for cool stars. Piskunov et al. (1990), though, compared the attributes of the

two functions in recovering known artificial images and concluded that the Tikhonov regularization had the advantage that it did not produce small, high contrast features below the spatial and temporal resolution of the data as tended to happen with maximum entropy regularization, a behaviour which they say was “typical” of maximum entropy images.

$$f = \sum_i Flux_i \ln(Flux_i) \quad (4)$$

An alternative approach to the problem of imposing an arbitrary form of regularizing function on the solution is the Occamian approach discussed in Berdyugina (1998). The main advantages advanced for this approach are that it avoids the a priori selection of some regularizing function that will, in the case of noisy data, produce some bias in the image. It is also advanced that the Occamian process naturally produces estimates of the error of the image elements. This argument, though, is disputed by Piskunov & Kochukhov (2002) who point out that error estimates can be obtained using any minimization technique since a variance of the image pixels can be estimated from the elements of the inverse of the main diagonal of the curvature (or Hessian) matrix.

While Piskunov Tuominen & Vilhu (1990) have shown that very aggressive application of the regularizing functions

can produce substantial qualitative differences in the images, ordinarily the choice of regularizing function has little effect on the image if the original data is of good quality and the fit to the data is at the level of the formal error.

2.2. The surface mapping parameter

There are two general approaches to the choice of how to describe the surface of the star. Codes by Piskunov and by Rice (see Piskunov & Rice 1993) and Berdyugina (1998) all map in surface effective temperature. Jankov & Foing (1992) and Vogt et al. (1987, 1999) map with some variation of surface flux which is thresholded in the case of Vogt et al. Collier-Cameron (1992), Donati & Brown (1997) and the Kurster (1993) codes work with a two temperature mode where they limit the model to a photospheric temperature and a spot temperature. In the case of Kurster the inversion process is different than those described above and is identified as a CLEAN-like algorithm. It amounts to a back projection of the data to provide a rough probability that any given pixel is part of a spot. Only one pixel at a time is identified as the most probable pixel to belong to a spot and it is chosen in the first iteration and assigned the spot temperature. Subsequent spot pixels, based on the residual profiles D/D_i where i is the iteration number and D the profile data, are chosen in subsequent iterations.

2.3. Converging on the geometric and atomic parameters

The stellar inclination, $v \sin i$, micro and macroturbulence are typically estimated to begin with and then refined based on successive runs of the imaging programs to find the values of these parameters that minimize the error in the fit to the observed profiles. The abundance of computing power now allows many runs to find the best fits, first minimizing based on one parameter, then minimizing another and cycling repeatedly through the values of the factors that are not mapped but that affect the fit to the observed profiles. In using photometric colours we find that the first parameters that must be adjusted are the stellar abundances since these affect the star colour in the sense that the mapping programs must adjust temperature to fit the profiles and the temperatures required to fit the profiles will be determined by the abundance of the elements producing the lines used in mapping. Thus small errors in abundance will leave the program unable to match the observed average colour of the star unless this is sorted out first.

Successive runs with trial errors of i and $v \sin i$ must then be run to find values of these parameters that minimize the error function. Fig. 3 is an example of the appearance of a plot of error-of-fit against differing adopted values of inclination of the rotational axis of the star for different image recoveries.

2.4. Including photometry

Piskunov & Rice (1993) discuss DI where photometric information is combined with the spectroscopic data to constrain the image. Since the χ^2 for the spectroscopic data and that for the photometry are vastly different and the photometry with

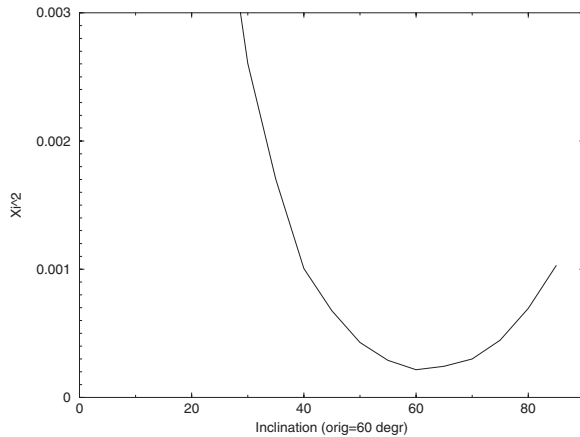


Fig. 3. An example of the sum of the squares of the residuals divided by the number of profile points in total for a range of inversion runs with different assumed inclination of the rotational pole for the star. This is an example from Rice & Strassmeier (2000) based on tests run on an artificial star where the original inclination was 60 deg.

its considerably poorer resolving power but generally much greater χ^2 will dominate the convergence unless given lower weight, the usual approach is to modify Eqn. 2 to be:

$$E = \chi_{\text{spec}}^2 + \beta \chi_{\text{phot}}^2 + \alpha f \quad (5)$$

and the purpose of the β is to allow for appropriate weighting of the photometric data. The task of actually integrating the flux through the appropriate photometric bandpass complete with filter weighting, line blanketing and adjusting for the standard calibration of photometry against standard stars is huge. Thus, in practice, the logarithm of continuum flux at band centre is calibrated against the standard magnitudes for stars of the same effective temperatures as the atmospheres provided to the code for the computation of the tabulated grid of line profiles. A spline fit is made to this calibration curve for purposes of interpolating to find appropriate magnitudes from the calculated intermediate logarithm of continuum flux for the model. A similar procedure for fitting the log of the ratio of the continuum fluxes at photometric band centre to the colours for the standard stars and then using the calibration curve to estimate the equivalent colour for the image from the log of the ratio of the calculated continuum fluxes of the recovered images can be practiced for the purpose of matching reconstructed to observed colour. This results in constraining the average temperature of the imaged star and, as mentioned above, is the basis for setting the abundance correctly. The weakness in this procedure is that the assumption made for each colour estimate is that the imaged star is, like the standard stars, homogeneous over its surface. While this is clearly untrue, the simple test of using band centre calculations given in Piskunov & Rice (1993), for example, suggests these fairly crude approximations are adequate. The use of combined spectroscopy and photometry has been used extensively by Strassmeier & Rice (e.g. Strassmeier et al. (1992) for LQ Hya) and by Unruh et al. (1995). Hendry & Mochnacki (2000) also used this approach to their modeling of close binaries with both spectroscopy and photometry.

2.5. Multiple line image recovery

With the expansion of computing power, the tendency is now to fit not just the time dependent variations of a single line but instead to recover images from multiple lines in the full observed spectrum. An example of this can be seen in Rice & Strassmeier (2001) in obtaining images of the young Pleiades star HII 314. The multi-line approach can be done on a line-by-line basis or by fitting all lines of the spectrum simultaneously. If this process is done separately on lines spread throughout the spectrum then errors of poor continuum placement, scattered light, wrong atomic parameters and random external errors can be screened to a degree by intercomparing the many images obtained to look for major inconsistencies. Alternatively, if we fit the full spectrum simultaneously we can use the odd-even tactic where images created from the odd phases of a data set are compared with those developed from the even phases to reveal features that arise largely through external errors in the data.

A variation on the utilization of the full spectrum directly, a variation called Least Squares Deconvolution, where a mean single profile is first obtained from the full spectrum, will be discussed later. This technique is now used in magnetic Doppler imaging.

The complete basic atomic data needed to exploit full spectral regions is available from the Vienna Atomic-line Database (VALD; Piskunov et al. 1995).

3. Tests of surface temperature mapping

3.1. Errors of image recovery and the artifact concern

In Berdyugina (1998) and in Piskunov & Kochukhov (2002) there are references to determining the theoretical errors for surface pixels based on the curvature of the error ellipsoid. Berdyugina has maps of the inversion error that arise from her Occamian approach to DI and these show, as one would expect, that the errors are less along the sub-solar line and toward the visible pole. For an ideal recovery, in the parts of the star along the extremum of visibility opposite the visible pole where the surface is only infrequently seen and when seen is only observed very obliquely the error is greatest as would be expected. The equatorial regions where we know the differentiation in latitude is poor we see greater error than for the region of about 75 degrees around the visible pole. Test cases of recovery from artificial data have long shown that there is only the strongest of features that can be recovered at the extremum of visibility opposite the visible pole and that features near the equator are smeared by the lack of velocity discrimination with latitude that arises from the rotation of a spherical star (see for example Rice, Wehlauf & Khokhlova 1989).

The major problem with a purely theoretical treatment of errors of recovery is that it basically presumes that major reduction errors in the spectrum or significant errors in factors used in reconstruction such as the inclination, the rotational velocity, atomic parameters or the failure of LTE etc. are absent. It is the errors in our images that are due to an incorrect

choice of $v \sin i$ or, in the case of the more slowly rotating stars, errors in local profile shape as a result of NLTE effects or mistaken macroturbulent velocity that give the most disturbing artifacts in our recovered images. One of the most striking differences in the images of active stars compared with solar activity is the appearance of large polar spot features, sometimes simply as high latitude features but in many cases as huge spots or dark caps extending over the entire rotational pole. Another, less commonly observed feature is the appearance of “hot spots” where there are significantly elevated temperatures over the “quiescent” photosphere. In some of the DI techniques, the image is forced to a two temperature solution, as mentioned above, so that the hot spots cannot appear since the authors are very concerned that in the free temperature solution it is too easy to get these hot spots.

The appearance of the cap features has significant implications for the dynamo processes that give rise to stellar activity and to issues of magnetic braking early in the evolutionary history of a star. The hot spot features may arise in T Tauri stars through an accretion process from the circumstellar disk onto the surface of the star or perhaps generally as huge faculae. Here I will deal with the extent to which these features can be trusted and leave the discussion of the physics of the features to others for now.

3.2. Empirical treatment of errors in image recovery

The earliest tests of Doppler imaging were designed to look for the effects of misjudgments in the selection of parameters such as $v \sin i$, inclination, gravity, initial starting temperatures and choice of regularizing function or the S/N level on the quality of the recovered image. With $v \sin i$ it was both a matter of the effect of an error in $v \sin i$ on the recovered image but also the lower values of $v \sin i$ that would allow us to obtain a useful image. Given the width of the local line profile at the stellar surface and the resolution of the spectrograph, $v \sin i$ determines the number of resolution elements on the recovered image. This becomes particularly important with young main-sequence stars. The pre-main-sequence stars and the post-main-sequence active stars such as the RS CVn stars typically are both fairly bright and have fairly high $v \sin i$ but given our desire to make comparisons with stars that approach the Sun in mass and that will potentially shed light on the early rotational braking phase of solar evolution, there is a need to look at many examples of these young main-sequence stars of roughly solar mass. Unfortunately these stars are faint in general and even the faster rotators have $v \sin i$ of only about 20 km s^{-1} (with the notable exception of AB Dor with $v \sin i$ of about 91 km s^{-1}). That implies that we have a special interest in objects that have rather large signal-to-noise and low $v \sin i$ and we are interested in what steps can be taken to minimize the incidence of polar spot and “hot spot” artifacts.

Numerous papers over the last fifteen years have given examples of recovered images from line profiles that have been calculated from a known image and then various errors have been introduced into the recovery. These include Vogt,

Penrod & Hatzes (1987), Rice, Wehlau & Khokhlova (1989), Piskunov & Wehlau (1990, 1994), Jankov & Foing and Donati & Catala (1993) among the earlier papers. More recent papers include Berdyugina (1998), Unruh & Cameron (1995, 1997), Bruls, Solanki & Schussler (1998) and Rice & Strassmeier (2000). Some of these have dealt specifically with the polar spot controversy.

3.2.1. Minimum $v \sin i$

The issue of minimal spectral resolution or minimum $v \sin i$ for useful DI was discussed in Piskunov & Wehlau (1990). They looked at resolutions ranging from 20,000 to 50,000 and considered $v \sin i$ at 15 km s^{-1} and 30 km s^{-1} . At the lowest spectral resolution and with $v \sin i$ of 30 km s^{-1} they could still accomplish reasonable recovery for the coarse features and similarly for the highest resolution and $v \sin i$ of 15 km s^{-1} . This work focussed on Ap star mapping. In general in cool star work the non-polar spot features are not as coarse as the abundance map features of Ap stars but their paper still offers reasonable guidelines for the limits on rotation speed and resolution. The lowest $v \sin i$ used so far is 18.0 km s^{-1} for the star AG Dor (Washuettl & Strassmeier 2001).

3.2.2. Abundance affect

The temperatures recovered for the stellar surface can be affected by the choice of $\log(gf)$, abundance for the element of the particular line used in the recovery (if there is only one line as opposed to a multi-line approach) or surface gravity error. This problem is brought under better control by incorporating photometric colour data into the recovery process. Forcing the stellar colour to follow observed $V - R_c$ or $b - y$ colours allows us to develop confidence in the abundances or $\log(gf)$ values and to bring the photospheric temperature to values consistent with observed colours as a preliminary step before the final iterations to obtain the published stellar image. The effect of being able to use the photometry to re-establish photospheric temperature consistent with the original artificial star even when other errors are forced on the recovery process is evident in Rice & Strassmeier (2000). The temperatures of the spots, though, are difficult to establish because the spots contribute very little to the total flux. One answer to this is to use molecular lines in the process. The contribution of the molecular lines will be concentrated in the spots and will partially offset the lack of flux. This is an approach that is just now being developed.

3.2.3. Phase gaps in data

Rice & Strassmeier (2000) responded to issues raised by referees who reviewed applications for observing time. The issues concerned in particular the size of phase gaps that could be tolerated in observing runs before the data became useless. For Ap star work missing phases are less serious since subsequent observing runs can fill in missing data given that the surface maps for these stars do not change in any short time

scale. This is not the case for cool stars and with large telescope time doled out in short three or four night runs, if the loss of one night means all is lost, the referees show concern. Issues such as spectrograph performance become important here too so issues of S/N and scattered light were investigated also. The conclusions on phase gaps in the data were clear that gaps of up to 100 deg were tolerable and produced losses in the image detail at and around the longitudes of the lost phases but the images for S/N = 300 were still useful.

3.2.4. Spot location

Generally there is agreement that the locations of spots are not significantly altered by errors in recovery parameters. The longitudes are most robust since that is a function of when the effect of the spot in the profile crosses line centre. Conclusions about spot preferred longitude should be quite reliable. The latitude of imaged spots is reasonably stable also. Errors in inclination or $v \sin i$ have some effect on the latitude but the effect is mostly the consequence of the modulation of the temperature profile of the spot by a global gradient induced by an error in a geometric or atomic parameter used in the recovery. It is universally apparent also that where observational noise is ideal Gaussian photon noise the effect of the noise on the image is simply to blur the image rather than to produce distortions in spot location. In fact, Rice & Strassmeier as well as some of the other authors have shown that useful results can be obtained with S/N of 150 and even at 75 there is some (albeit rather blurred) major elements of the original image still evident. This was with cases of $v \sin i$ of 28 km s^{-1} and 41 km s^{-1} . The problems of S/N are usually more serious for very rapidly rotating stars where surface resolution might be better in principle because of the greater velocity dispersion associated with features over the surface of the star but counterbalancing that is the much shallower line profiles that become very sensitive to S/N. The mapping information is contained in the depth of the line profile so that line profiles that have been reduced in depth to a few percent of continuum are severely damaged by reduced S/N. Once $v \sin i$ exceeds about 100 km s^{-1} the S/N requirements become very large.

There have now been a number of papers drawing major conclusions about differential rotation, spot lifetimes and spot drift based on extended Doppler imaging runs. A few examples of assessing differential rotation through direct tracking of spots are: AB Dor (Collier-Cameron, Donati & Semel 2002), PZ Tel (Barnes, Collier-Cameron, James & Donati 2000), HU Virgo (Strassmeier 1994; Hatzes 1998), KU Peg (Weber & Strassmeier 2001), UX Ari (Vogt & Hatzes 1991), HR 1099 (Vogt & Hatzes 1996), EI Eri (Hatzes & Vogt 1992) IL Hya (Weber & Strassmeier 1998) and V410 Tau (Rice & Strassmeier 1996). HR 1099 has been monitored in long runs by both Strassmeier & Bartus (2000) and by Vogt et al. (1999). They both report a stable polar cap and lifetimes of the order of a month or so for smaller spots distant from the polar cap. The possibility that these smaller non-polar spots drift toward the pole over their lifetime is an intriguing suggestion from these papers.

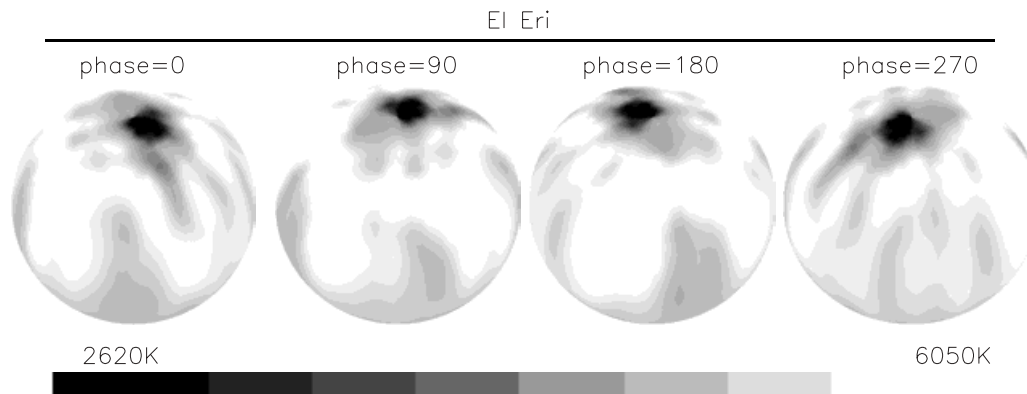


Fig. 4. An image of EI Eri developed from the line profiles of Fig. 5. Basically one of the images from Strassmeier et al. (1991) but rendered differently here.

3.3. Polar cap spots

In the early days of developing Doppler images large polar cap features were discovered on stars such as EI Eri (e.g. Strassmeier 1990). The initial reaction among many was that these must be artifacts. The principle reason for the doubt about the polar spots was that the large polar cap spots do not exhibit wavelength variability in their effect on the observed profile as a result of the star's rotation. Errors in the determination of the local line profile shapes used for the inversion could produce axisymmetric features such as polar caps or bands of flux parallel to the lines of latitude on the surface of the stars.

Earlier Unruh & Collier-Cameron (1995) had run tests on artificial star data and simulated the effect of several parameter errors but those that seemed to have the most effect were errors in choice of radial-tangential microturbulent velocity and unrecognized blends. Substantial error in the radial-to-tangential component of microturbulence seemed to produce a fairly smooth gradient in the filling factor toward the pole (although it was hard to interpret in terms of temperature variation). The tests were run with a fairly large $v \sin i$ value of 50 km s^{-1} . They restricted their test to recovery without attempting to adjust the $v \sin i$ for a minimum and they seem to suggest they believe that would have reduced the gradient they observed (and I believe that would certainly be true). They showed much greater concern for the effect of unrecognized blends which produced significant equator-to-pole gradients in the image. While a potentially very serious form of error I believe that a multi-line approach to imaging would minimize this particular problem. Images formed from sections of spectra that contain many lines or separate images from several different lines that are averaged together will suppress the effect of blends or spurious atomic parameters that might appear in images from some of the individual lines.

Berdyugina (1998) alludes to the tendency to get a polar gradient in the temperature distribution on a stellar surface if the $v \sin i$ was in error by 2 km s^{-1} or more for stars with $v \sin i$ of about 50 km s^{-1} . Again, the effect is fairly low contrast in comparison with the more sharply defined features seen on the likes of EI Eri or HD 199178. (See Fig. 4 for an image of EI Eri and Fig. 5 for the line profiles.)

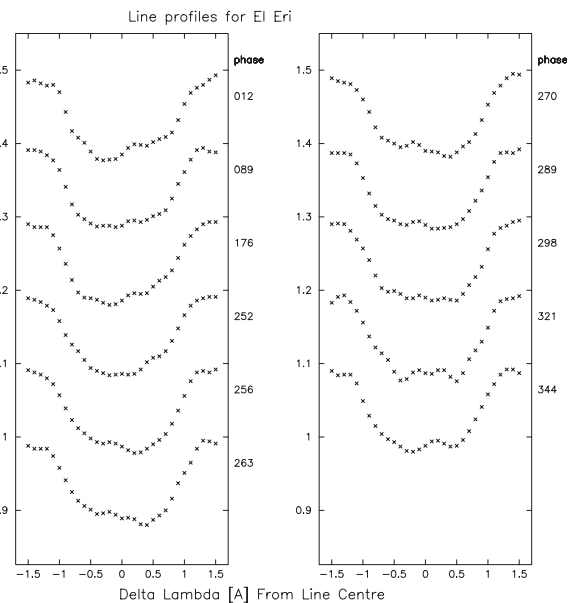


Fig. 5. The wide, flat bottom line profiles of the RS CVn star EI Eri.

Several papers have dealt specifically with the issue of whether polar cap features are artifacts. Unruh & Collier-Cameron (1997) checked for the effect of emission in the cores of the Na D lines on AB Dor images that were produced from these lines as compared with images from three weak photospheric lines. They used local line profiles from a template star and a two temperature approach. The comparison indicated, contrary to what one would expect, that images from the Na lines with possible core emission showed *less* evidence of high latitude spot features than appeared in the images from the three weaker photospheric lines.

The possibility that errors in local line shape due to assumptions of LTE in the calculation of these local profiles has been frequently discussed as a potential source of spurious polar caps. Bruls, Solanki & Schussler (1998) computed NLTE profiles for a set of commonly used DI lines. They suggested that only a few would show core infilling that would significantly affect rotationally broadened profiles. Piskunov et al. (2001) though have done a careful calculation with the Ca 6439Å line in NLTE and show NLTE effects can seri-

ously affect the appearance of the polar feature. In contrast, for stars such as HD 199178 (Strassmeier et al. 1999; Hackman, Jetsu & Tuominen 2001) *all* lines, including weak ones where NLTE effects are not significant, show the flat bottom profiles indicative of the presence of a large and deep polar spot.

As an alternative to a complete polar cap, Hackman et al. (2001) explore the suggestion that a very large anti-solar differential rotation along with a high latitude polar spot can mimic the effects of polar caps. They can, in fact, produce very flat bottomed profiles but only by using extremely large differential rotation ($\alpha = -0.17$) along with a large high latitude spot. They, however, still argue that this gives a better fit to the line profiles. The attempt to explain the appearance of a polar cap in images of the T Tauri star Sz 68 by differential rotation led Johns-Krull & Hatzes (1997) to conclude that solid body rotation with a polar cap was the better solution. Generally, reviews of the differential rotation observed through monitoring long lived spots do not give large values for α (see Hatzes 1998). The fairly large value estimated for α on KU Peg by Weber & Strassmeier (2001) is not anti-solar in nature. While these measurements of differential rotation suggest that eliminating the appearance of polar caps by assuming large anti-solar differential rotation is not a viable alternative to polar caps for most stars exhibiting flat bottom profiles, clearly the discussion of the reality of polar caps is not closed.

While there are still doubts raised about individual cases, it seems that the general consensus now is that large polar cap spots do exist on many of the observed stars. Indeed, now theory seems to permit spots to appear at the pole in stars with deep convection zones and rapid rotation (Schusler & Solanki 1992). There is even the hypothesis that stars with residual rapid rotation may be those where the predominant exit point for the magnetic flux is polar and hence the braking action that would have led to rapid loss of angular momentum was less effective. This leaves the star with continued high angular momentum at a stage of evolution when this ordinarily would have disappeared.

3.4. Bright, hot spots

Even more contentious, and with less written about it, is the issue of localized bright or hot spots on the surfaces of some stars. To illustrate that hot artifacts can appear I have prepared Fig. 6. This is an artificial star with no hot spots in the original. When line profiles are calculated for a low $v \sin i$ of 20 km s^{-1} and a low macroturbulent velocity of 2 km s^{-1} and then recovery is accomplished with a much larger, perhaps unrealistic, macroturbulence of 6 km s^{-1} , we can see a hotter area adjacent to one of the dark spots in the image. The temperature of the “hot spot” in this extreme example is only about 250 K. The feature arises because the local line profiles for recovery are substantially different than those used in the original calculation of the profiles. Some accommodation for the wider profiles in recovery was made by way of adjusting the $v \sin i$ downward, but I suspect I could have recovered the image with less temperature in the “hot spot” if I had minimized the error of fit by doing the usual search for minimum

error with $v \sin i$. Nonetheless, this serves as an indication of the way spurious features of this sort can appear. Since I have deliberately chosen a $v \sin i$ that is at the lower limit of those used for DI and a fairly substantial error in a factor such as macroturbulence, this probably represents the extent of such artifacts in size and temperature deviation but this problem has not been fully explored.

At the other end of the problem, when “hot spots” are in existence, are they adequately rendered in the Doppler images? In Rice & Strassmeier (2000) we inverted multiple images with “hot spots” at varying latitudes to see to what degree they had been distorted. The initial spots were 500 K above the surrounding photosphere and Fig. 7 and Fig. 8 illustrate the results. Note too, in these figures, with the higher $v \sin i$ of 28 km s^{-1} and 41 km s^{-1} that the spurious hotter spots that occur in the areas immediately surrounding deep cool spots do not have temperatures that approach in level the temperature of the “real” hot spot which is at 500 K. Typically the spurious hot spots (the artifacts) can be described as a) having the character of “rebound” features near large cool spot regions and b) tend to have temperature elevations of no more than about 200 K above the photosphere.

Papers with reference to hot spots that seem to fit the category of “real” are the very bright regions on DF Tau, a CTTS, where a two temperature approach has been used by Unruh, Collier-Cameron & Guenther (1998) in creating images of hot spots. The image development was performed in two stages where, in the first instance, the photosphere was represented as at 3750 K and the hot spot temperature was adopted as 5500 K, i.e. 1750 K hotter than the photosphere. In the second stage the cool spot image was created from the de-veiled spectrum. If the hot spots have no line absorption of significance, the effect of hot spots in producing moving “bumps” in the line profiles is very similar to the effect of cool spots. Great care was taken in this publication to clearly identify which effects arose (amidst the veiling) from hot spots and which was due to cool features. In the case of the WTTS V410 Tau, Rice & Strassmeier (1996) recovered features at 500 K above the photosphere which appear to be real.

3.5. The double-blind test

Ideally the best test of Doppler imaging is a test in which the very difficult issues of external errors of observation as well as all the differences of individual codes, techniques, spectrographs and all that is in the pipeline between star and image on the paper is tested by having observations and reconstruction runs that are done independently and unknowingly by two different researchers. There was a test where the same star was observed at the same time at two different observatories and its image produced with no interaction between the authors. Such a test did occur accidentally with the observations of V410 Tau in 1993 by Hatzes (1995) and by Rice & Strassmeier (1996). A comparison of the two images, appropriately modified to adjust for the direction of rotation, the zero of phase and the image scale being different, is presented here in Fig. 9. V410 Tau is a fairly rapidly rotating T Tauri star so the issue of whether the high latitude spot features are an artifact of both images is not in question here.

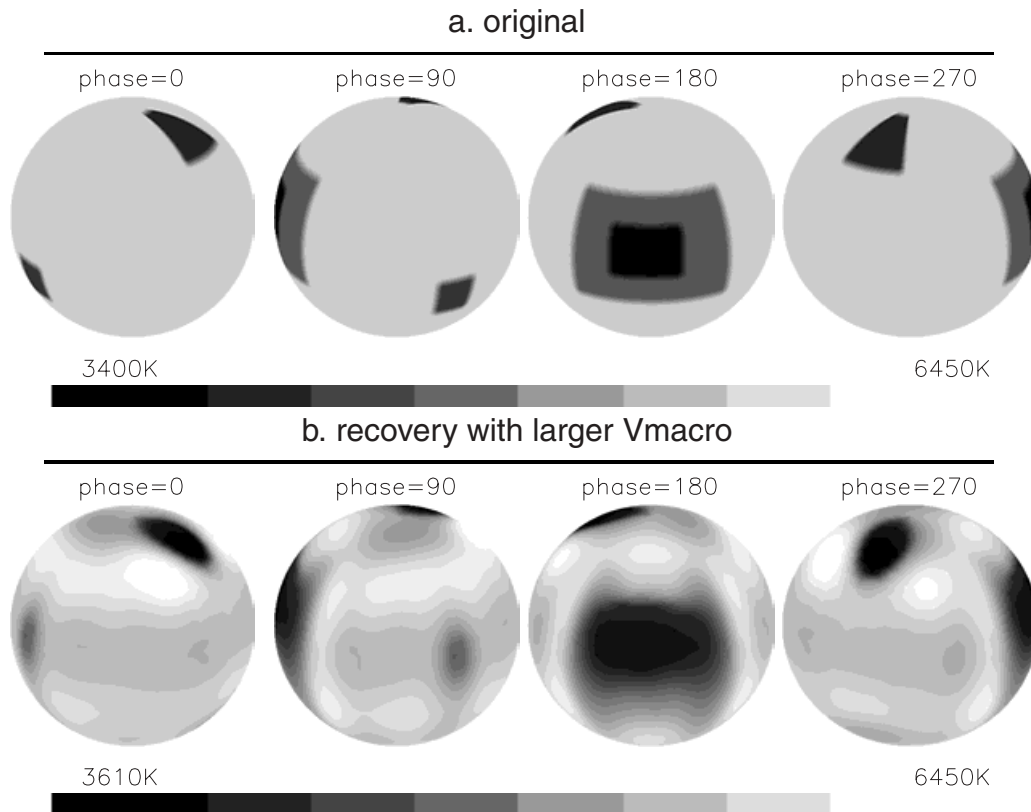


Fig. 6. Recovery of an image when V_{macro} is very much higher on recovery than in the original artificial image. The line profile for the original was calculated with $V_{\text{macro}} = 2.0 \text{ km s}^{-1}$ and the recovery of panel b was with $V_{\text{macro}} = 6.0 \text{ km s}^{-1}$. This example is for a small $v \sin i$ case.

The images compare very well in spite of the differences in technique and display. More significant perhaps is the comparison between the two publications in terms of the basic parameters adopted. $V \sin i$ was found to be 77 km s^{-1} in both cases but the adopted values for i were very different. Hatzes used a value of $i=54 \text{ deg}$ and Rice & Strassmeier used a value of 70 deg . The use of photometry in the Rice & Strassmeier image is the apparent source of the differences seen in mean temperature on the left side of the two images as shown in Fig. 9.

Another interesting test where exactly the same data on the star EI Eri was independently distributed to three sets of Doppler imagers is displayed in Strassmeier et al. (1991). The images developed for this rapidly rotating RS CVn star showed very good agreement, even though the data set had been developed from different spectrographs.

4. Binary star images

Hendry & Mochnacki (2000) and Maceroni et al. (1994) have tackled the very challenging task of DI of contact binary systems. For these systems the geometry of the surface shape and the division of the surface into elements becomes very difficult. I will not attempt to review this work but recommend it to you as very thorough work indeed. In the case of non-eclipsing, non-contact binaries that are clear double line binaries, tidally locked and where the stars are not more

than one or two percent different from a sphere in shape, it is not too difficult to generalize DI programs to simultaneously create images of both stars from spectra and photometry representing the entire cycle of the stars. I have done this and Strassmeier & Rice (2002) are producing images of $\sigma^2 \text{ CrB}$ from CFHT Gecko spectra and photometry from the automated photometric telescopes.

One interesting aspect of the test figures we have done for the paper is that the behaviour of the program in rendering an image of the fainter star of the binary pair is to display reduced resolution compared to the brighter star that contributes more signal. This is consistent with the single star behaviour and illustrates how the process is inclined not to produce spurious surface detail, even when faced with limited S/N and a penalty function application that is appropriate to the S/N of the brighter star.

5. Magnetic Doppler imaging

In principle there is no problem producing a Doppler image of a star in terms of the distribution of surface temperature/abundance and magnetic field vector. We simply generalize the minimization of Equ. 2 so that now we minimize an equation of the form of Equ. 6.

$$E = \chi_I^2 + \chi_Q^2 + \chi_U^2 + \chi_V^2 + \alpha \cdot f \quad (6)$$

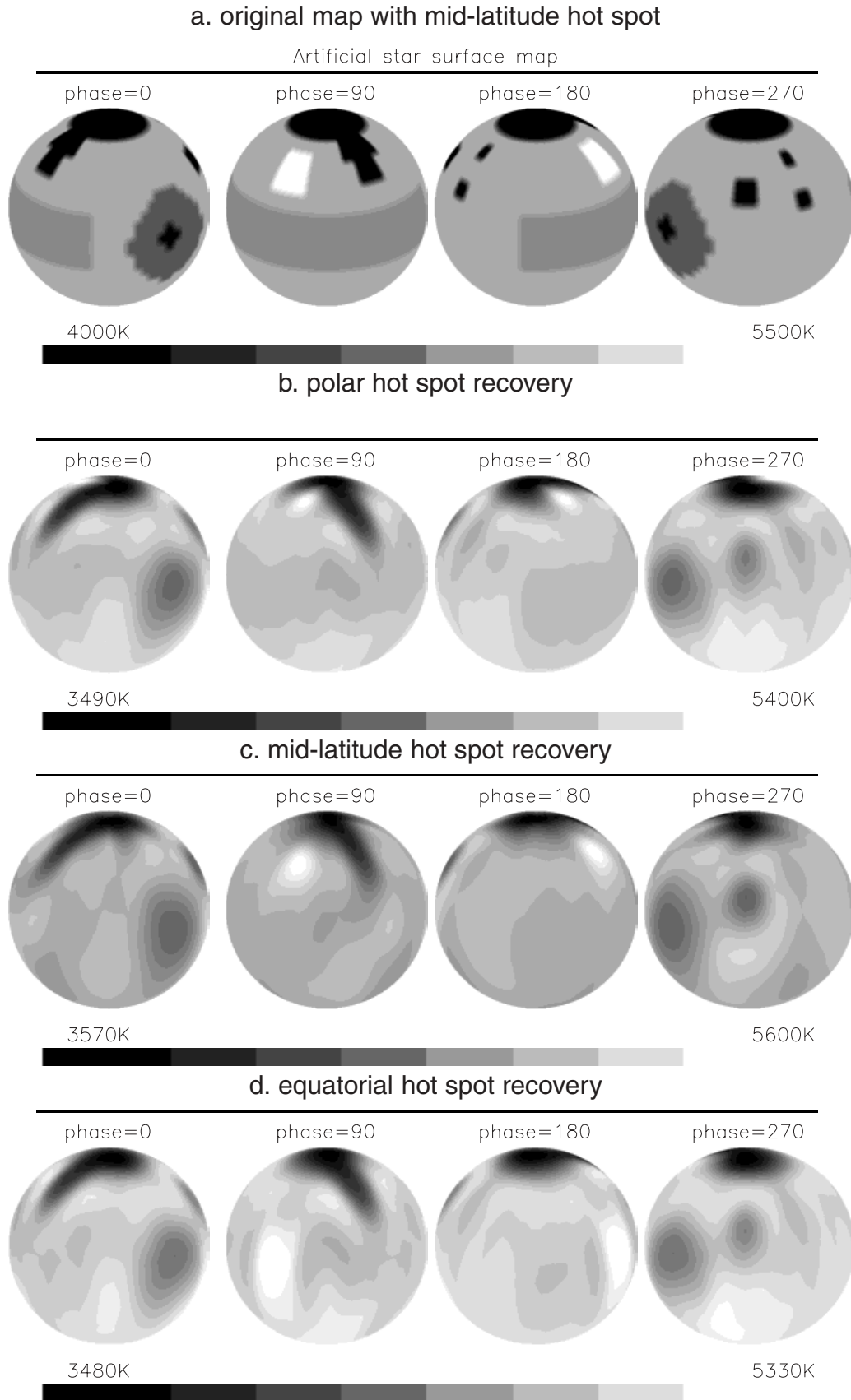


Fig. 7. Recovery of hot spots at various latitudes for an artificial star with inclination of 65 degrees, $v \sin i$ of 28 km s^{-1} and S/N of 300.

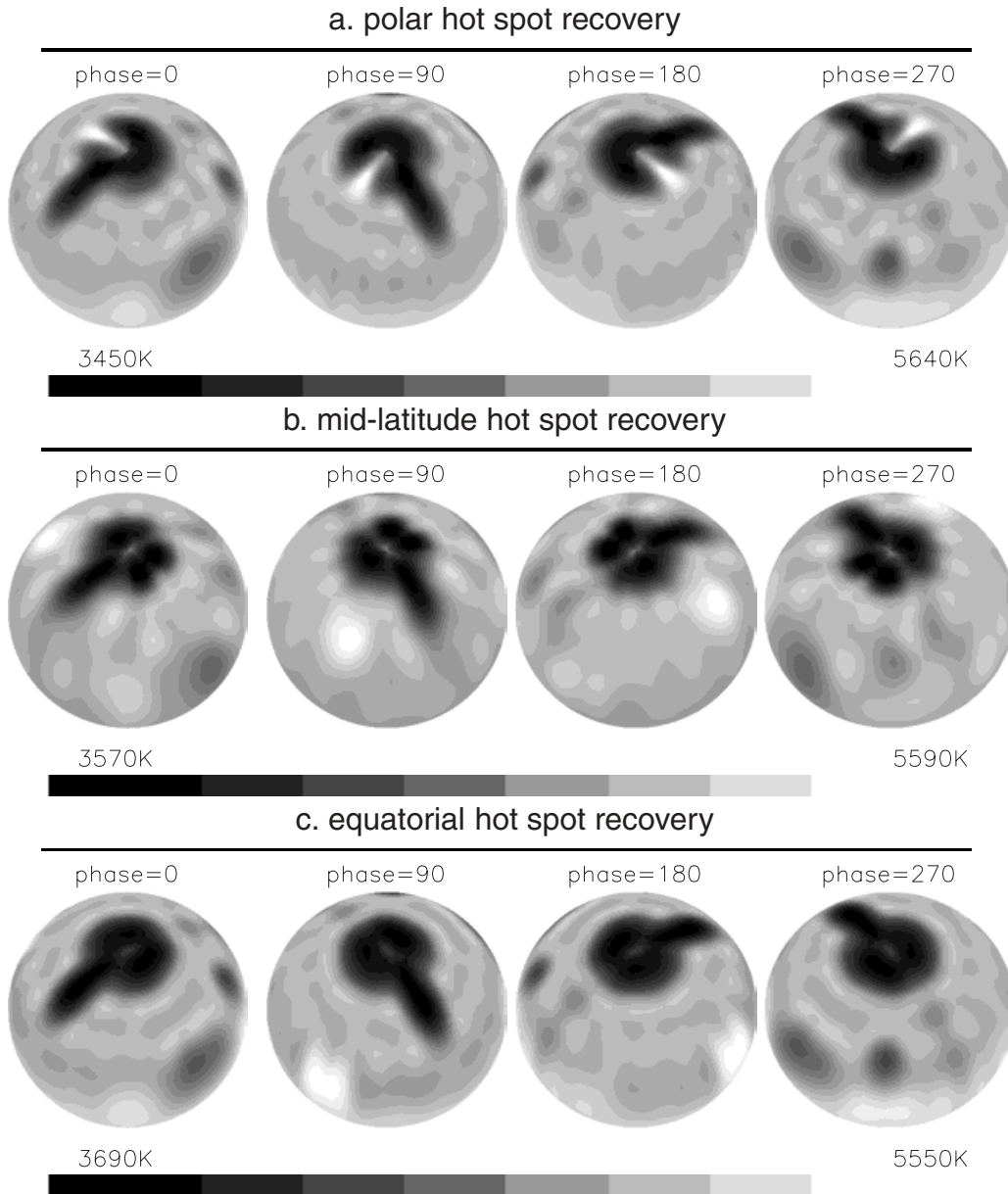


Fig. 8. Recovery of hot spots at various latitudes for an artificial star with inclination of 30 degrees and $v \sin i$ of 41 km s^{-1} .

Here χ_Q^2 would mean:

$$\sum_{\phi} \sum_{\lambda} \frac{1}{\sigma_{Q,\lambda,\phi}^2} [Q_{calc,B,T}(\lambda, \phi) - Q_{obs}(\lambda, \phi)]^2 \quad (7)$$

and $Q_{calc,B,T}(\lambda, \phi)$ represents the calculated Q at each wavelength and phase for a given surface distribution of the magnetic field (B) and temperature (T). In practice the divergent choice of parameters for representations of B on the stellar surface, the large difference in the scale of I, Q, U and V in observation and the difficulties of either imposing a global field distribution or choosing a form of regularization complicate the minimization considerably.

Along with the development of conventional Doppler imaging came the hope of ultimately using spectra fully observed in all Stokes parameters (or at the very least, observations in both I and V) to simultaneously resolve both the surface temperature (or abundance) distribution and the cause

of these effects, the magnetic field, where the field would appear as a distribution of both field strength and orientation. Progress here is much slower for a number of reasons. First, the signal level in V is typically no more than a few tenths of a percent and the Q and U signal level much lower still. To simply observe the magnetic signature is difficult but to use Q, U and V observations for mapping would require getting S/N in the Q, U and V signal of perhaps a hundred so that the I of the observations used to determine the Q, U and V must have S/N of the order of several thousand. This is very challenging for a single line observation but might be accomplished using multiple line observations. Second, the tabling techniques used in conventional Doppler imaging to reduce computing demands are not readily accomplished if line profiles from actual model atmospheres are to be used in the imaging process. Reasonable estimates of the number of profile calculations required for tabling shows that the comput-

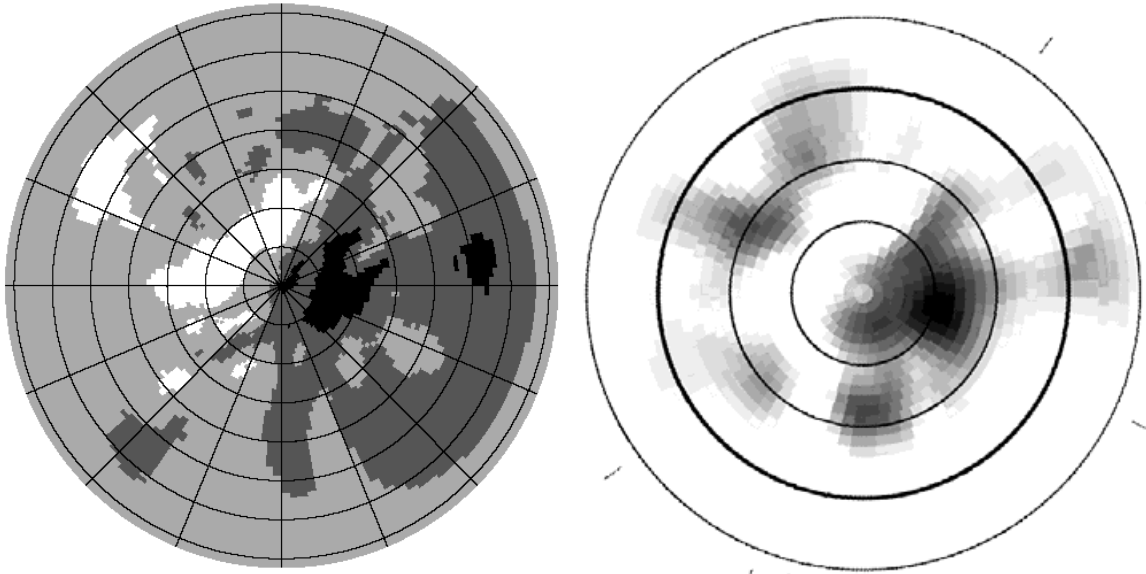


Fig. 9. A comparison between two images of V410 Tau obtained at approximately the same time but developed using different telescopes, different programs and different workers operating completely independently. The independent work concluded the same $v \sin i$ exactly but the value of i was adopted as 70 deg for the image by Rice & Strassmeier (1996) on the left and for the image by Hatzes (1995) on the right i was set at 54 deg. In spite of the significant difference for i , the completely independent images show very good agreement. The lower contrast features in the upper left of the Hatzes image are probably suppressed in the image by Rice & Strassmeier by the inclusion of photometry in the code used by Rice & Strassmeier.

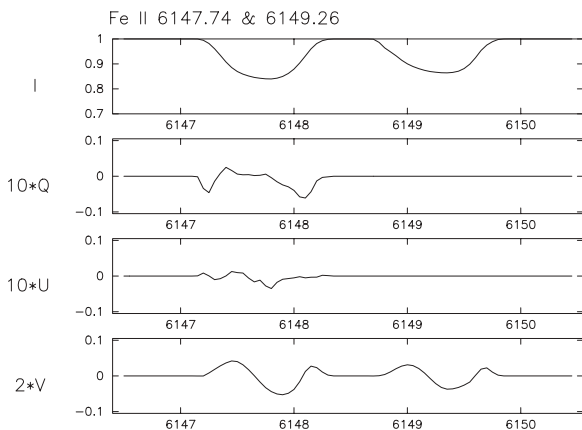


Fig. 10. A comparison of IQUV values (integrated over a uniform hot star surface) for two lines of Fe II, 6147.74Å and 6149.26Å. The point of this figure is that the V profiles for the two lines are almost identical and depend on surface features and rotational velocity whereas the Q and U are very different for the two lines.

ing effort to table is quite comparable to, and perhaps greater than, recalculating the profile as needed. This requires that for every iteration of the inversion, the line profile in all Stokes parameters has to be calculated for every element of the stellar surface for as many phases as observed and repeated for as many separate calculations of the error as are used in minimizing that iteration (in a conjugate gradient technique). Further, the gradient calculation also requires numerous repetitions of the profile calculations. While numerical procedures such as DELO (Rees, Murphy & Durrant 1989) have been utilized to speed this up, it is still a massive computing problem requiring some form of parallel processing. Third, the

question of the difficulty of obtaining enough signal from the surface elements that produce little flux (or, in the case of Ap stars, that have very weak lines) to clearly determine global field is an interesting and debatable issue. In principle weak lines are produced with a Zeeman splitting that would always reveal the local field but the signal level in the observed profile becomes potentially very low, even lower than the very low signal already discussed. Finally, there are issues of indeterminacy in the components of the local field unless global constraints such as forcing the field to be a dipole or dipole/quadrupole field structure is imposed a priori for stars such as the Ap stars.

5.1. The signal level in Q, U and V and Least Squares Deconvolution

The issue of the very low signal level in the Stokes spectra of individual lines is perhaps the most serious obstacle to creating reliable images of stars with both the temperature and magnetic field resolved. Semel (1989) outlined the idea of improving the S/N in polarimetric measurements by averaging the measurements of many lines. Semel's work basically presumes observations of the I and V Stokes parameters although he does envision reconstruction of images from all four Stokes parameters. He proposes that the field structure on the stellar surface is encoded in these mean profiles and the idea that the surface can be mapped from the mean profile data is inherent in his paper. Donati, Semel, Carter, Rees & Collier-Cameron (1997) implement this idea by using what they have called Least Squares Deconvolution (LSD) to ex-

tract the mean I and V profiles from thousands of lines in echelle spectra. Essentially they create a mask function

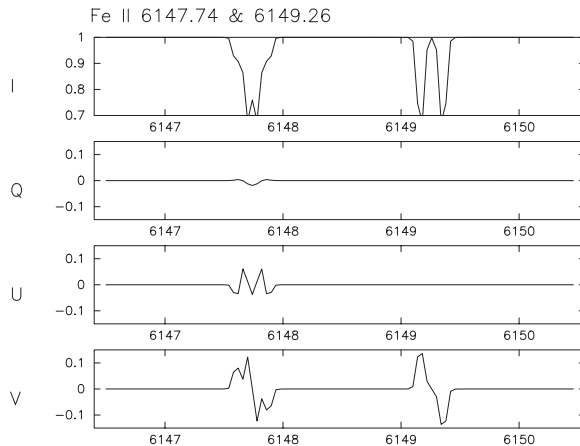
$$P(v) = \sum_i w_i \delta(v - v_i) \quad (8)$$

where w_i and v_i are the weight for each spectral line and the position in units of velocity for the lines to be averaged in the spectrum. This mask is convolved with the mean V Zeeman signature, Z , for lines in the spectrum ($V = P * Z$) to represent the actual circularly polarized spectrum of the star. A least squares procedure is adopted to extract Z from a fit of V to the observed spectrum and the errors associated with each pixel of the mean Zeeman signature. They point out that the process is essentially an improved version of a deconvolution of V with P , including in the process the errors of the pixels of the original spectrum, to produce Z and to get error bars for the pixels of Z . The effect is to get a mean V profile (Z) that has far higher S/N and that displays the phase dependent profile features characteristic of the temperature and magnetic distribution over the surface of the star. One can see from Fig. 10 that the disk integrated V pattern for lines of differing quantum numbers is quite similar in V so this becomes a practical answer to the very low signal level in V for individual lines. Further, since the computing time required to calculate detailed profiles, one at a time, for all the lines in a very large wavelength region is excessive, attempts to solve the S/N problem with multi-line calculations are doomed and LSD appears to be the only answer to the low signal level issue at this time. Donati et al. (1997) comment on the potential for extending Least Squares Deconvolution to the I spectrum for very faint sources but say little about application to Q and U although there are implications in some comments that there is potential for application to Q and U. Clearly, from just the simple illustration in Fig. 10, the application of LSD to extracting useful mean profiles for Q and U will require some form of binning to accommodate the divergence of Q and U profiles with J, L and S for the upper and lower levels of the transitions. Thus, because of the generally larger V signal (especially for the Ap stars) and because of the increased difficulty of applying LSD to Q and U data, observations with the I and V data have dominated magnetic DI for the last decade.

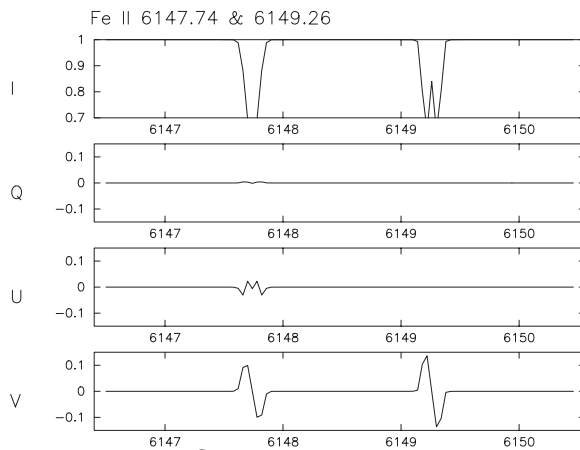
5.2. The computing problem and magnetic mapping redundancy

While the code for a full model atmosphere based magnetic DI solution requires vast computing resources, there have been a number of improvements suggested to speed up the tedious calculation of the Stokes spectra including magneto-optical effects. One of the fastest is DELO, developed by Rees, Murphy & Durrant (1989) along with a suggested improvement to DELO to increase accuracy made by Socas-Navarro, Trujillo & Ruiz (2000). Other procedures for rapid computing of the Stokes parameters with speed and accuracy comparisons are discussed in Piskunov & Kochukhov (2002). Even with the improved algorithms for calculating the local I, Q, U, V profiles, the computing task for a full model atmosphere and full recalculation of every local line profile in its

a. Field at 4kG



b. Field at 2kG



c. Field at 1kG

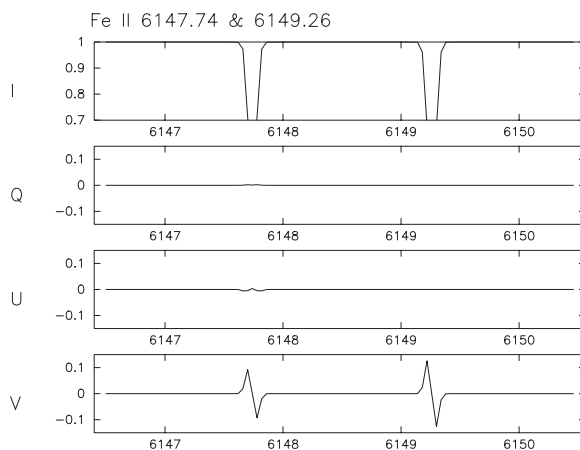


Fig. 11. The local line intensity as seen from almost vertically over the surface of a dwarf star of $T_{\text{eff}} = 9000$ K for two Fe II lines displayed in all four Stokes parameters. The three displays are at different magnetic field strength with the orientation of the magnetic field at about 50 degrees to the line of sight. With a field under about 2 to 3 kG, changing the local field strength is roughly equivalent to changing the local light flux contribution to the integrated V profile since there is little variation in the local V profile shape with field strength below 3 kG.

full Stokes representation is so huge that reasonable computing times, even with fast processors requires that we take advantage of the natural parallelism in the problem and use devices such as clusters of computers and MPI (Message Passing Interface) to distribute the task over many processors. I have found that even with a fast single processor system, a code I developed that imposes a global dipole/quadrupole with full I,Q,U,V recalculation for every surface element can take weeks for enough iterations for a proper minimization.

Various simplified approaches to creating images from I and V data were tried as initial explorations of the problem. Brown, Donati, Rees & Semel (1991) used a line formation model due to Landolfi & Landi Degl'Innocenti (1982) that assumes a plane parallel Milne-Eddington model atmosphere and a constant ratio between line centre and continuum absorption coefficients and a Planck source function. They tested recovery of magnetic structure over test stars with radial magnetic fields alone for both uniform and spotted brightness distribution. They also tested magnetic distributions of spotted and dipole configurations. With a recovery procedure that also assumes a radial local field orientation they find, somewhat similarly to the recovery in non-magnetic Doppler imaging, that spots of positive and negative field strength on a surface of uniform brightness are recovered better near the polar regions and less accurately near the equator. A pair of tests where the forward test case was calculated with a dipole field and either just a radial component or both radial and tangential components and recovery using radial components alone gave similar results in terms of recovery. The magnetic field recovery for uniform brightness distribution showed rather poor recovery in the sense of surface longitude. Poor recovery of the dipole field is attributed to the significant loss of sensitivity in the V profiles to the radial field information from the heavily limb darkened limb regions. This is less of a problem for the highly localized fields of spotted stars where the V data as the spot passes the sub-solar meridian will highlight the longitude of the spot feature better than a field structure with more widely distributed strong field components such as the dipole field. It is because of this result that there is a sense that magnetic structure on the surface of Ap stars, where the field has been presumed to be a low order multipole configuration, should have a dipole/quadrupole configuration imposed on the field as part of the reconstruction process. From the work of Bagnulo, Landolfi & Landi Degl'Innocenti (1999) it appears that this should be approached with caution since they find only some of the stars they have studied appear to have fields of such low order. Again, in Bagnulo (2001) the message is that in many cases for the Ap stars the field can be represented by a dipole/quadrupole combination but that there are also many exceptions where, at the very least, a higher order structure is present.

Subsequently, Donati & Brown (1997) revisited the issue of recovering field structure from Stokes I and V data. In this paper they assumed Gaussian line profiles and that the magnetic splitting would be a Zeeman triplet with a common Lande factor. They tested models with field orientation specified by the full three spherical coordinate values, radial,

azimuthal and meridional (this term was used to mean a component tangent to the surface and directed toward the pole). The local Stokes V signatures of individual lines were assumed to be modulated only in amplitude. This assumption arises from a phenomenon that is illustrated in Fig. 11, i.e. that since the local line width smears the Stokes V profiles, up to a magnetic field strength of several thousand Gauss the width of the V signature is fairly constant although its amplitude will vary with magnetic field strength. This means that the amount of contribution to the total integrated line profile from each surface element depends on the field strength and the surface intensity but the shape of the contribution is basically the same. Only for large fields does the shape of the local V signature vary with field strength and atomic transition.

The general approach for spotted star simulation in Donati & Brown (1997) was to adopt spots that had fields of 500G confined to a sharply defined spot. They tested field orientations that were pure radial, meridional or azimuthal. The significant issues that arise from these tests is that the behaviour of the shape of the surface integrated V signature over the rotational cycle for an azimuthal field is basically antisymmetric around the meridian passage of the spot while the behaviour of the V signature for the spots with radial or meridional field was symmetric. For spots at high latitude there was sufficient distinction in behaviour, even for the radial versus meridional spots that some clear resolution of the three components could be established in the reconstruction but for the more equatorial spots the radial vs. meridional resolution was very uncertain so that crosstalk was a serious problem. The conclusion was that magnetic DI from I and V had good potential for resolving azimuthal versus radial-meridional field components and a number of papers have presented images of azimuthal as distinct from the radial-meridional component. Examples are AB Dor (Hussain, Donati, Collier-Cameron & Barnes 2000), HR 1099 and LQ Hya (Donati 1999). An interesting characteristic of these maps is the strong widespread azimuthal component of field over the surface, in the case of AB Dor this is concentrated in rings around the pole.

An interesting proposal that is a variation on direct magnetic DI (or Zeeman Doppler Imaging - ZDI as it is often called) is in the paper by Hussain, Jardine & Collier-Cameron (2001). They propose and test modeling the magnetic potential field as opposed to the the magnetic induction field B.

5.3. Observation and reconstruction with IQUV

Observations in all four Stokes parameters are beginning to appear. An atlas of the visible spectrum of β CrB in IQUV has appeared (Wade, Donati & Landstreet 2000). The atlas covers most of the visible spectrum and will be useful in planning future observations with instruments capable of extracting full Zeeman signatures. A paper with IQUV spectra and model simulations of the spectra of the Ap stars β CrB and 53 Cam are published in Bagnulo et al. (2001). Full reconstructions of surface abundance/temperature/brightness and magnetic structure based on the complete IQUV are only now

on the verge of appearing in the literature. Donati (2001) still argues that it is not possible to unambiguously recover the global fields of Ap type stars, even with full IQUV.

Piskunov & Kochukhov (2002) have published a paper on techniques of calculating images from IQUV and of recovering the magnetic field in a global sense in the most difficult situation, i.e. Ap stars. The paper has very interesting comparisons of differing computational approaches to both minimization and to the precision and speed of calculating the Zeeman split local line profile using DELO, Feautrier etc. on different grid density for the model atmosphere. Perhaps the most interesting aspect of the paper is the regularization they are using, a regularization they refer to as multipolar regularization. They actually do use some Tikhonov regularization in their procedure but the emphasis in their paper is on a regularization that is based on real spherical harmonic expansions. The magnetic field at each iteration is fitted with a harmonic expansion to impose smoothing and the resultant final spherical expansion representing the field can be converted to a dipole, quadrupole etc. representation of the field. In this paper, without abundance variation over the stellar surface, Piskunov & Kochukhov present examples of recovering the full global field without having the crosstalk problem between the radial and meridional components discussed above. In the test cases discussed here, the polar field is set at 8 kG and so the information available in the IQUV spectra from the test maps is greater, with detail in the QUV spectra less buried in the thermal width of the local line profiles. In a conference paper (Piskunov 2001) the same procedural approach is used for recovering the image of a test star where there is an abundance variation in the form of a spot with enhanced abundance and not only does Piskunov recover the global field but he says that the procedure works for stars with $v \sin i$ as low as 10 km s^{-1} . Results for applying this technique to α^2 CVn are also given.

6. Summary

It would appear that the state of the development of conventional non-magnetic Doppler imaging is becoming mature to the extent that now it is a matter of obtaining long enough runs on stars of interest that spot lifetimes, migrations, differential rotation and indeed, even stellar activity cycles, can be deduced for stars in successive evolutionary states. Artifacts are still a problem in image recovery but our experience with conventional DI is now great enough for us to make reasonable suppositions about what is real and what is an artifact of the image recovery process. For magnetic Doppler imaging the issues of how best to cope with the limitations on observation of IQUV spectroscopy because of low signal level and the potential problems of crosstalk between the recovered radial and meridional/polar-tangential components of the magnetic field in global field recoveries, such as with the Ap stars, is still problematical.

Acknowledgements. I would like to thank the Natural Sciences and Engineering Research Council of Canada for ongoing support of my research.

References

- Barnes, J., Collier-Cameron, A., James, D., Donati, J-F.: 2000, MNRAS 314, 162
- Bagnulo, S.: 2001, in: S. Mathys, S. Solanki, D. Wickramasinghe, (eds.), *Magnetic Fields across the HR Diagram*, ASP Conf. Ser. 248, 287
- Bagnulo, S., Landolfi, M., Landi Degl'Innocenti, M.: 1999, A&A 343, 865
- Bagnulo, S., Wade, G., Donati, J-F., Landstreet, J., Leone, F., Monin, D., Stift, M.: 2001, A&A 369, 889
- Berdyugina, S.: 1998, A&A 338, 97
- Brown, S., Donati, J.-F., Rees, D., Semel, M.: 1991, A&A 250, 463
- Bruls, J., Solanki, S., Schussler, M.: 1998, A&A 336, 231
- Collier-Cameron, A.: 1992, in: P. Byrne, D., Mullan (eds.), *Surface inhomogeneities on late-type stars*, Springer-Verlag, Berlin, p. 33
- Collier-Cameron, A., Donati, J-F., Semel, M.: 2002, MNRAS, in press
- Donati, J-F.: 2001, in: H. Boffin, D. Steeghs, J., Cuypers, (eds.), *Proc. of the First International Workshop on Astro-Tomography*, Springer, Berlin
- Donati, J-F.: 1999, MNRAS 302, 457
- Donati, J-F., Brown, S.: 1997, A&A 326, 1135
- Donati, J-F., Catala, C.: 1993, A&A 277, 123
- Donati, J-F., Semel, M., Carter, B., Rees, D., Cameron, A.: 1997, MNRAS 291, 658
- Goncharski, A., Stepanov, V., Khokhlova, V., Yagola, A.: 1977, SvAL 3, 147
- Goncharski, A., Stepanov, V., Khokhlova, V., Yagola, A.: 1982, SvA 26, 690
- Hackman, T., Jetsu, L., Tuominen, I.: 2001, A&A 374, 171
- Hatzes, A.P.: 1995, ApJ 451, 784
- Hatzes, A.: 1998, A&A 330, 541
- Hatzes, A., Vogt, S.: 1992, MNRAS 258, 387
- Hendry, P., Mochnecki, S.: 2000, ApJ 531, 467
- Hussain, G., Donati, J-F., Collier-Cameron, A., Barnes, J.: 2000, MNRAS 318, 961
- Hussain, G., Jardine, M., Collier-Cameron, A.: 2001, MNRAS 322, 681
- Jankov, S., Foing, B.: 1992, A&A 256, 533
- Johns-Krull, C.M., Hatzes, A.P.: 1997, ApJ 487, 896
- Kurster, M.: 1993, A&A 274, 851
- Landolfi, M., Landi Degl'Innocenti, E.: 1982, SoPh 78, 355
- Maceroni, C., Vilhu, O., van't Veer, F., Van Hamme, W.: 1994, A&A 288, 529
- Piskunov, N.: 2001, in: S. Mathys, S. Solanki, D. Wickramasinghe, (eds.), *Magnetic Fields across the HR Diagram*, ASP Conf. Ser. 248, 293
- Piskunov, N., Kochukhov, O.: 2002, A&A 381, 736
- Piskunov, N., Kupka, F., Ryabchikova, T., Weiss, W., Jeffery, C.: 1995, A&AS 112, 525
- Piskunov, N., Rice, J.B.: 1993, PASP 105, 1415
- Piskunov, N., Tuominen, I., Vilhu, O.: 1990, A&A 230, 363
- Piskunov, N., Vincent, A., Duemmler, R., Ilyin, I., Tuominen, I.: 2001, in: R.J. Garcia Lopez, R. Rebolo, M. Osorio (eds.), *11th Cambridge workshop on cool stars, Stellar Systems and the Sun*, ASP Conf. Ser. 223, 1285
- Piskunov, N., Wehlau, W.H.: 1990, A&A 233, 497
- Rees, D., Murphy, G., Durrant, C.: 1989, ApJ 339, 1093
- Rice, J.B., Strassmeier, K.G.: 1996, A&A 316, 164
- Rice, J.B., Strassmeier, K.G.: 2000, A&AS 147, 151
- Rice, J.B., Strassmeier, K.G.: 2001, A&A 377, 264
- Rice, J.B., Wehlau, W.H., Khokhlova, V.: 1989, A&A 208, 179

- Rice, J.B., Wehlau, W.H., Khokhlova, V., Piskunov, N.: 1981, in: *Upper Main-Sequence Chemically Peculiar Stars*, 23rd Liege Astrophysics Coll., p. 265
- Schussler, M., Solanki, S.K.: 1992, A&A 264, L13
- Strassmeier, K.G.: 1990, ApJ 348,682
- Strassmeier, K.G.: 1994, A&A 281, 395
- Strassmeier, K.G., Bartus, J.: 2000, A&A 354, 537
- Strassmeier, K.G., Lupinek, S., Dempsey, R.C., Rice, J.B.: 1999, A&A 347, 212
- Strassmeier, K.G., Rice, J.B.: 2002, A&A, in preparation
- Strassmeier, K.G., Rice, J.B., Wehlau, W.H., Hill, G., Matthews, J.: 1992, A&A 268, 671
- Strassmeier, K.G., Rice, J.B., Wehlau, W.H., Vogt, S., Hatzes, A., Tuominen, I., Piskunov, N., Hackman, T., Poutanen, M.: 1991, A&A 247, 130
- Semel, M.: 1989, A&A 225, 456
- Skilling, J., Bryan, R.: 1984, MNRAS 211, 111
- Socas-Navarro, H., Trujillo Bueno, J., Ruiz Cobo, B.: 2000, ApJ 530, 977
- Tikhonov, A.: 1963, Sov. Math. Dokl. 4, 1624
- Unruh, Y., Collier-Cameron, A.: 1995, MNRAS 273, 1
- Unruh, Y., Collier-Cameron, A.: 1997, MNRAS 290,L37
- Unruh, Y., Collier-Cameron, A., Cutispoto, G.: 1995, MNRAS 277, 1145
- Unruh, Y., Collier-Cameron, A., Guenther, E.: 1998, MNRAS 295, 781
- Vogt, S., Hatzes, A.: 1990, in: I. Tuominen, D. Moss, G. Rüdiger (eds.), *The Sun and Cool Stars: Activity, Magnetism, Dynamos* IAU Coll. 130, Springer-Verlag, p. 297
- Vogt, S., Hatzes, A.: 1996, in: K.G. Strassmeier, J. Linsky, (eds.), *Stellar Surface Structure*, IAU Symp. 176, Kluwer Publ., p. 245
- Vogt, S., Hatzes, A., Misch, A., Kurster, M.: 1999, ApJS 121, 547
- Vogt, S., Penrod, G., Hatzes, A.: 1987, ApJ 321, 496
- Wade, G., Donati, J-F., Landstreet, J.: 2000, NewA 5, 455
- Weber, M., Strassmeier, K.G.: 1998, A&A 330, 1029
- Weber, M., Strassmeier, K.G.: 2001, A&A 373, 974
- Washuettl, A., Strassmeier, K.G.: 2001, A&A 370,218